SUMOylation-Dependent LRH-1/PROX1 Interaction Promotes Atherosclerosis by Decreasing Hepatic Reverse Cholesterol Transport

Stein, Sokrates; Oosterveer, Maaike H.; Mataki, Chikage; Xu, Pan; Lemos, Vera; Havinga, Rick; Dittner, Claudia; Ryu, Dongryeol; Menzies, Keir J.; Wang, Xu

Published in:
Cell metabolism

DOI:
10.1016/j.cmet.2014.07.023

Cell Metabolism
Article

SUMOylation-Dependent LRH-1/PROX1 Interaction Promotes Atherosclerosis by Decreasing Hepatic Reverse Cholesterol Transport

Sokrates Stein,[1] Maaike H. Oosterveer,[2] Chikage Mataki,[1] Pan Xu,[1] Vera Lemos,[1] Rick Havinga,[2] Claudia Dittner,[3,4] Dongryeol Ryu,[1] Keir J. Menzies,[1] Xu Wang,[1] Alessia Perino,[1] Sander M. Houten,[5] Frauke Melchior,[3] and Kristina Schoonjans[1,*]

[1]Metabolic Signaling, Institute of Bioengineering, School of Life Sciences, Ecole Polytechnique Fédérale de Lausanne, 1015 Lausanne, Switzerland

[2]Department of Pediatrics, Center for Liver Digestive and Metabolic Diseases, University of Groningen, University Medical Center Groningen, 9700 RB Groningen, the Netherlands

[3]Zentrum für Molekulare Biologie Heidelberg (ZMBH), DKFZ-ZMBH Alliance, 69120 Heidelberg, Germany

[4]Joint Division Molecular Metabolic Control, Zentrum für Molekulare Biologie Heidelberg, Deutsches Krebsforschungszentrum (DKFZ) and University Hospital Heidelberg, DKFZ-ZMBH Alliance, 69120 Heidelberg, Germany

[5]Department of Genetics and Genomic Sciences, Icahn School of Medicine at Mount Sinai, New York, NY 10029, USA

*Correspondence: kristina.schoonjans@epfl.ch

http://dx.doi.org/10.1016/j.cmet.2014.07.023

SUMMARY

Reverse cholesterol transport (RCT) is an antiatherogenic process in which excessive cholesterol from peripheral tissues is transported to the liver and finally excreted from the body via the bile. The nuclear receptor liver receptor homolog 1 (LRH-1) drives expression of genes regulating RCT, and its activity can be modified by different posttranslational modifications. Here, we show that atherosclerosis-prone mice carrying a mutation that abolishes SUMOylation of LRH-1 on K289R develop less aortic plaques than control littermates when exposed to a high-cholesterol diet. The mechanism underlying this atheroprotection involves an increase in RCT and its associated hepatic genes and is secondary to a compromised interaction of LRH-1 K289R with the corepressor prospero homeobox protein 1 (PROX1). Our study reveals that the SUMOylation status of a single nuclear receptor lysine residue can impact the development of a complex metabolic disease such as atherosclerosis.

INTRODUCTION

Atherosclerosis is a disease characterized by excessive cholesterol accumulation in vessel walls. It evolves from a complex interplay between hypercholesterolemia, dyslipidemia, and chronic inflammation and encompasses several tissues and organs (Weber and Noels, 2011). Rupture of an atherosclerotic plaque may lead to a myocardial infarction or stroke, two of the primary causes of morbidity and mortality in the world (Weber and Noels, 2011).

Liver receptor homolog 1 (LRH-1 or NR5A2) is a member of the NR5A subfamily of nuclear receptors (NRs) that binds as a monomer to its response elements (Fayard et al., 2004). The transcriptional activity of LRH-1 is governed by multiple factors, including the binding of ligands and posttranslational modifications, which together define its interaction with transcriptional coregulators (Fernandez-Marcos et al., 2011; Lee and Moore, 2008). LRH-1 is highly expressed in tissues of the enterohepatic axis, where it has diverse molecular and physiological functions (Fayard et al., 2004) ranging from local glucocorticoid production in the intestine (Coste et al., 2007) to glucose sensing in the liver (Oosterveer et al., 2012). Interestingly, one of the first described LRH-1 target genes is *scavenger receptor B type 1* (*Scarb1*) (Schoonjans et al., 2002), a gene that is expressed in many tissues and plays important functions in reverse cholesterol transport (RCT), an antiatherogenic process in which excessive cholesterol from peripheral tissues is transported to the liver and finally excreted via the bile (Rosenson et al., 2012). Although several other LRH-1 target genes involved in cholesterol metabolism have been identified, including *carboxl ester lipase* (*Cel*) (Fayard et al., 2003), *ATP binding cassette member subfamily G5* (*Abcg5*), *Abcg8* (Freeman et al., 2004), and *apolipoprotein M* (*Apom*) (Venteclef et al., 2008), so far no study has demonstrated that LRH-1 activity is critical for proper RCT or atherogenesis.

LRH-1 is targeted for SUMOylation by E3-SUMO ligases at several lysine residues, and this conserved reversible posttranslational modification affects its transcriptional activity (Chalkiadaki and Talianidis, 2005; Lee et al., 2005; Talamillo et al., 2013; Venteclef et al., 2010; Ward et al., 2013). SUMOylation of human LRH-1 is considered to attenuate its transcriptional activity, yet the mechanistic basis underlying this repression is poorly understood. Although one study reported that the SUMOylated form of LRH-1 is sequestered into promyelocytic leukemia (PML) protein bodies (Chalkiadaki and Talianidis, 2005), another study proposed that SUMO modification of LRH-1 stabilizes the recruitment of the transcriptional nuclear receptor corepressor 1 and histone deacetylase 3 (NCoR1/Hdac3) corepressor complex through its association with G protein pathway suppressor 2 (GPS2) (Venteclef et al., 2010).

In this study, we demonstrate that mice carrying a mutation on lysine 289 of LRH-1 (*Lrh1 K289R* mice) display reduced LRH-1

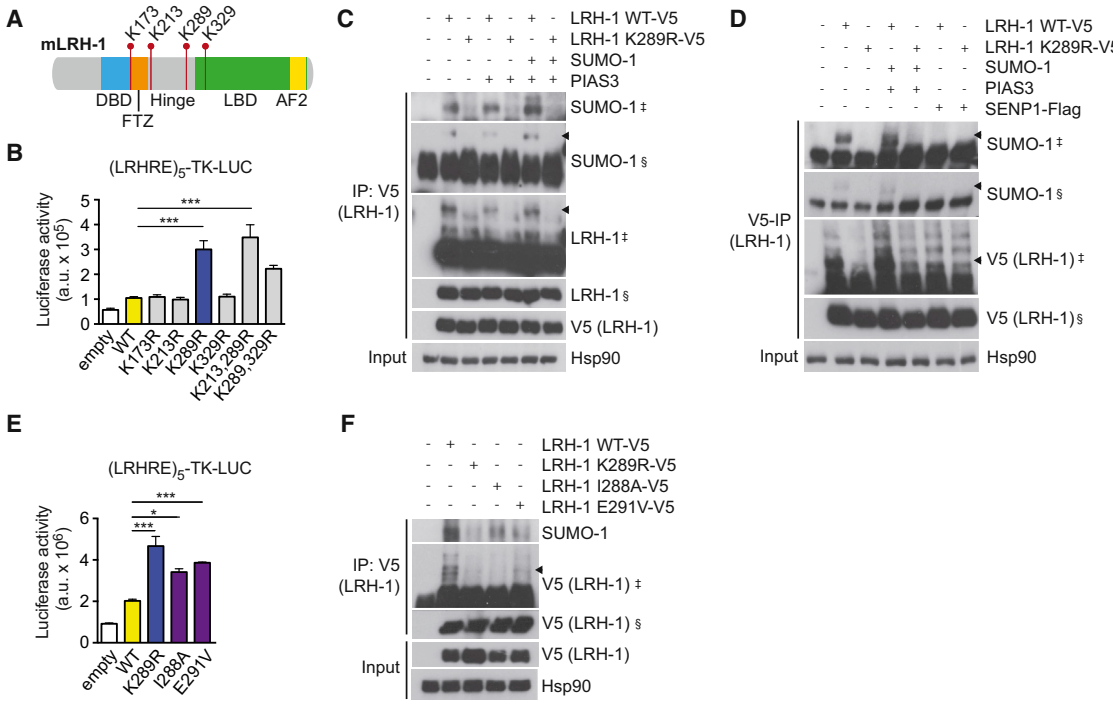

Figure 1. Non-SUMOylatable LRH-1 K289R Displays Increased Reporter Activity and Impaired SUMOylation In Vitro

(A) Schematic overview of LRH-1 highlighting the lysine residues that were mutated. DBD, DNA binding domain; FTZ, fushi tarazu homology domain; LBD, ligand binding domain; AF2, activation function 2 domain.

(B) Luciferase assay performed in HEK293T cells that were cotransfected with a pGL3::$(LRHRE)_5$-TK-LUC and a pCMV plasmid coding for LRH-1 WT or the outlined mutant constructs. n = 3. The experiment was replicated three times.

(C) Immunoprecipitation of V5-tagged LRH-1 to detect the SUMOylated band of LRH-1 (arrowheads). HEK293T cells were transfected with pCMV-V5::LRH-1 WT or pCMV-V5::LRH-1 K289R, pCMV::PIAS3, and/or pcDNA-HA::SUMO-1-HA. The experiment was replicated at least three times.

(D) Immunoprecipitation of V5-tagged LRH-1 to detect the SUMOylated band of LRH-1 in HEK293T cells that were transfected with pCMV-V5::LRH-1 (WT or K289R) and pCMV-FLAG::SENP1. The experiment was replicated at least three times.

(E) Residues adjacent to K289 are required for SUMOylation and function of LRH-1 activity. Luciferase assay was performed in HEK293T cells that were cotransfected with a pGL3::$(LRHRE)_5$-TK-LUC and pCMV plasmid coding for LRH-1 WT or the outlined mutant constructs. n = 3 from three separate experiments.

(F) Immunoprecipitation of V5-tagged LRH-1 to detect SUMOylation of the different mutant constructs used in (E).

Data are represented as means ± SEM. *$p < 0.05$, **$p < 0.01$, ***$p < 0.001$ relative to *Lrh-1 WT*, as determined by ANOVA and Bonferonni post hoc or Student's t test. Arrowheads, LRH-1*SUMO-1 band; §, short exposure; ‡,long exposure.

SUMOylation and increased expression of genes regulating cholesterol transport. When crossbred to atherosclerosis-prone *low-density lipoprotein receptor* (*Ldlr*) knockout mice, *Ldlr−/− Lrh-1 K289R* mice show improved RCT and diminished atherosclerosis development in comparison to control mice. Mechanistically, this effect is attributed to the specific loss of interaction of the mutated form of LRH-1 with the corepressor PROX1, thereby increasing the expression of LRH-1 target genes involved in RCT.

RESULTS

Non-SUMOylatable LRH-1 K289R Displays Increased Transcriptional Activity In Vitro

The murine LRH-1 protein has several lysine (K) residues that could be SUMOylated. They are located in the DNA binding domain, hinge region, or ligand binding domain (Figure 1A). On the basis of previous studies (Lee et al., 2005), we mutated the most relevant K residues to non-SUMOylatable arginines (R) and analyzed their potential to *trans*-activate a heterologous LRH-1 reporter by transient transfection assays (Figure 1B). Interestingly, the K289R mutation displayed the highest transcriptional activity, whereas the remaining K mutations (K173R, K213R, or K329R) had neither an effect as single mutations nor an additive effect when mutated together with K289R (Figure 1B). Next, we analyzed whether the enhanced activity of LRH-1 K289R was also associated with a reduction in the SUMOylation status. Human embryonic kidney 293T (HEK293T) cells transfected with either LRH-1 wild-type (WT) or LRH-1 K289R were cotransfected with either PIAS3 SUMO ligase alone or in combination with SUMO-1 substrate. Basal LRH-1 WT SUMOylation was clearly detectable, whereas it was nearly undetectable in LRH-1 K289R (Figure 1C). Cotransfection with PIAS3 and SUMO-1 slightly increased SUMOylation of LRH-1 WT (Figure 1C). Notably, LRH-1 K289R SUMOylation remained low after PIAS3 and SUMO-1 cotransfection, showing that mutating a single K residue can affect the total SUMOylation status of the transcription factor (Figure 1C). Moreover, cotransfection of LRH-1 WT or LRH-1 K289R with the isopeptidase sentrin/SUMO-specific protease 1 (SENP1) efficiently removed the SUMO modification from only LRH-1 WT (Figure 1D). The SUMO acceptor

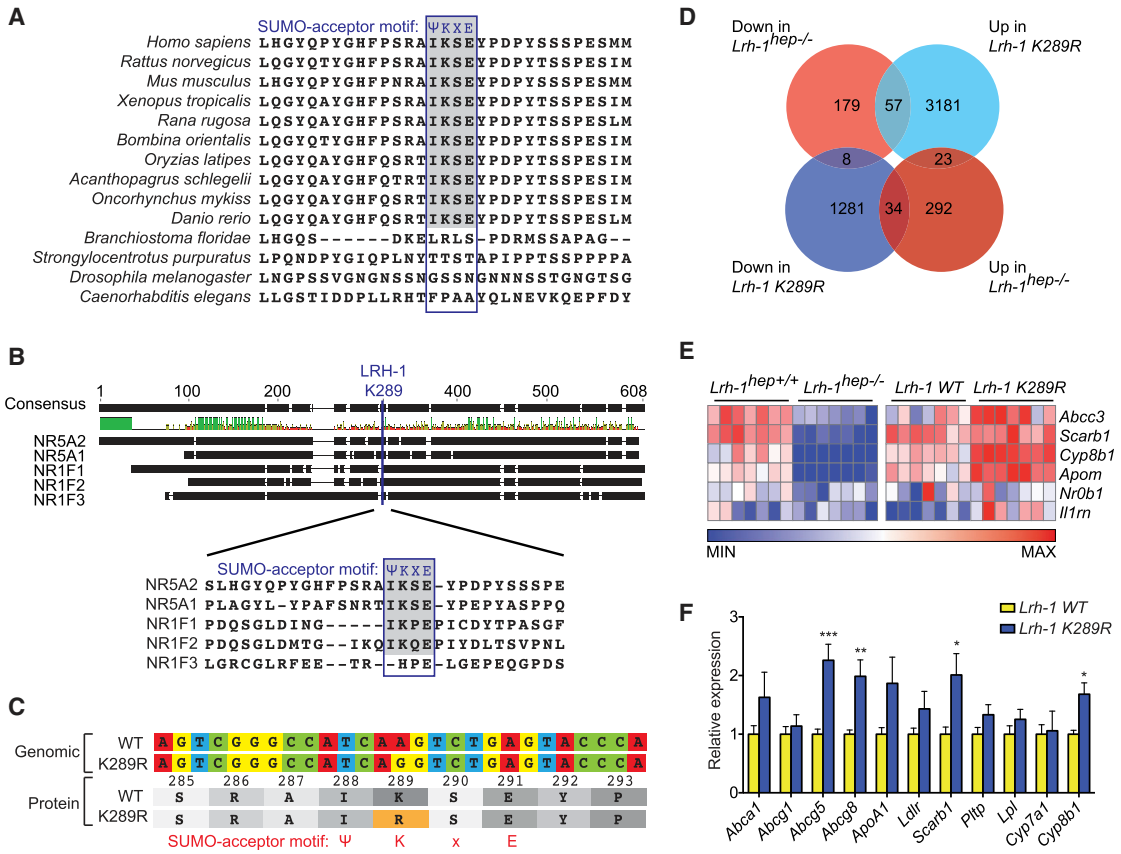

Figure 2. The LRH-1 SUMO Acceptor Motif Is Conserved in Vertebrates, and Mutation of Its Lysine Triggers Activation of Cholesterol Homeostasis Genes In Vivo

(A) Alignment of the amino acid sequence surrounding the murine LRH-1 K289 residue with other species. The blue-lined box highlights the aligned amino acids homologous to the SUMO acceptor motif, and the gray shading marks the sequences with an intact SUMO acceptor sequence.

(B) Protein alignment of LRH-1 (NR5A2) with other monomeric NR showing conserved sequences surrounding the LRH-1 K289 residue. Green, high homology; red, low homology.

(C) Overview of the genomic and protein sequence surrounding the K289R mutation. Mutation of a single nucleotide (AAG → AGG) at genomic level leads to K289R mutation of the translated protein.

(D) Venn diagram depicting the number of genes that are significantly up- or downregulated in *Lrh-1*$^{hep-/-}$ (n = 8) in comparison to *Lrh-1*$^{hep+/+}$ (Oosterveer et al., 2012) (n = 8) as well as *Lrh-1 K289R* (n = 7) in comparison to *Lrh-1 WT* (n = 7) mice.

(E) Heatmap displaying the expression of selected LRH-1 target genes in the corresponding genotypes (n = 4 per genotype).

(F) Hepatic expression of genes that regulate cholesterol homeostasis in *Lrh-1 WT* (n = 8) and *Lrh-1 K289R* (n = 9) mice.

Data are represented as means ± SEM. *p < 0.05, **p < 0.01, ***p < 0.001 relative to *Lrh-1 WT*, as determined by Student's t test. See also Figures S1 and S2.

motif Ψ-K-x-E is found in many SUMOylated proteins. Although the lysine residue can be targeted for SUMOylation, the adjacent hydrophobic (Ψ) and acidic glutamate (E) residues are also necessary to mediate the conjugation with the SUMO E2 enzyme Ubc9 (Bernier-Villamor et al., 2002). Mutation of these two sites (I288A and E291V) also increased LRHRE-driven reporter activity (Figure 1E) and reduced LRH-1 SUMOylation (Figure 1F), showing that not only the lysine but also an intact SUMO acceptor motif is crucial for the SUMO-dependent function of LRH-1.

LRH-1 K289R Activates Selected Target Genes In Vivo

To understand the relevance of this particular SUMO acceptor lysine residue, we carried out comparative alignment studies. Alignment of the amino acids surrounding the murine LRH-1 K289 with other species demonstrated that this particular SUMO acceptor motif is highly conserved in vertebrates but not in the chordate lancelet (*Branchiostoma floridae*), sea urchin (*Strongylocentrotus purpuratus*), fruit fly (*Drosophila melanogaster*), or roundworm (*Caenorhabditis elegans*; Figures 2A; Figure S1A available online). However, homologous proteins in *C. elegans* and *D. melanogaster* have other sites that can be targeted for SUMOylation (Talamillo et al., 2013; Ward et al., 2013). Next, we compared the murine LRH-1 protein sequence with other monomeric NRs with special focus on the highly variable and intrinsically disordered hinge region (Krasowski et al., 2008). Besides the close homolog NR5A1 (SF-1), only the retinoic-acid-receptor-related orphan receptors (RORs:NR1F1, NR1F2, and NR1F3) displayed somewhat homologous hinge regions (Figure S1B). Closer alignment of LRH-1 with NR5A1 and the three RORs showed that only NR1F1 and NR1F2 contain

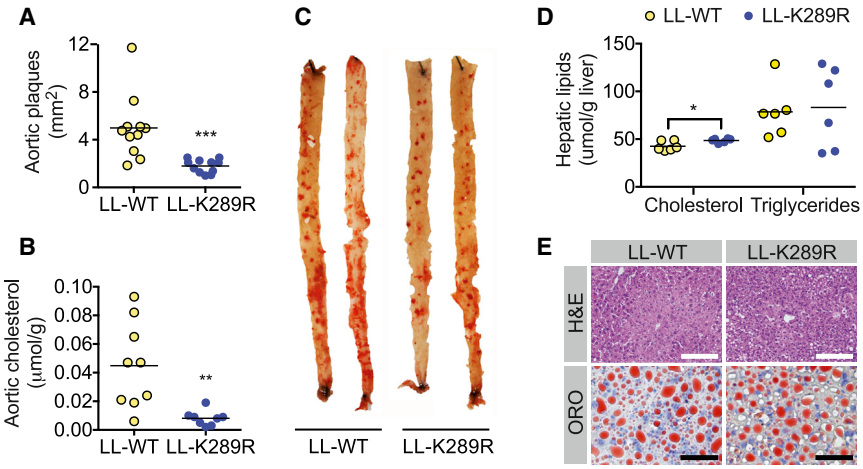

Figure 3. LRH-1 K289R Protects against Atherosclerosis Progression

(A) Quantification of aortic plaque area in *Ldlr*$^{-/-}$ *Lrh-1 WT* (LL-WT) or *Ldlr*$^{-/-}$ *Lrh-1 K289R* (LL-K289R) mice. n = 11 per genotype.

(B) Quantification of the cholesterol content in aortic lipid extracts of LL-WT (n = 9) and LL-K289R (n = 8) mice.

(C) Representative aortas of LL-WT and LL-K289R mice stained with Oil-Red O.

(D) Quantification of cholesterol and triglyceride contents in hepatic lipid extracts of LL-WT and LL-K289R mice. n = 6 per genotype.

(E) Representative images of hematoxylin and eosin and Oil-Red O (ORO) staining of hepatic sections of LL-WT and LL-K289R mice. The white scale bar represents 200 μm, and the black scale bar represents 50 μm.

Data are represented as means ± SEM. *p < 0.05, **p < 0.01, ***p < 0.001 relative to LL-WT, as determined by Mann-Whitney U or Student's t tests. See also Figure S3.

the conserved SUMO acceptor motif (Figure 2B). These bioinformatic data suggest that SUMOylation of this site is specific for a very small subset of NRs and highlights the functional importance of the hinge region in these selected NRs.

To analyze the physiological impact of the K289R mutation on LRH-1 function in vivo, we generated a knockin mouse line containing the K289R mutation *Lrh-1 K289R* (Figures 2C and S2A). The offspring of *Lrh-1 K289R* breeders were born under normal Mendelian and sex ratios, and no apparent dysmorphic phenotype could be observed in these mice (data not shown). The mutation did not affect the expression of LRH-1 in the liver in comparison to *Lrh-1 WT* and hepatocyte-specific *Lrh-1*$^{hep+/+}$ mice (Figure S2B). Then, we performed microarray analyses on livers in order to compare the transcriptome of hepatocyte-specific *Lrh-1*$^{hep-/-}$ (Oosterveer et al., 2012) and *Lrh-1 K289R* mice to their corresponding controls. Only 57 of the 244 genes (23.4%) whose expression was decreased in *Lrh-1*$^{hep-/-}$ mice were induced in *Lrh-1 K289R* mice (Figure 2D and Table S1). Several of the established LRH-1 target genes that are reduced in *Lrh-1*$^{hep-/-}$ mice were oppositely regulated in *Lrh-1 K289R* mice (Figure 2E). Intriguingly, most of the selected hepatic LRH-1 target genes involved in cholesterol metabolism were increased in *Lrh-1 K289R* in comparison to *Lrh-1 WT* mice, as determined by qPCR analyses (Figure 2F). Although hepatic expression of *Cyp8b1* was nearly absent in hepatocyte-specific *Lrh-1*$^{hep-/-}$ mice (Mataki et al., 2007), it was only mildly enhanced in *Lrh-1 K289R* mice (Figure 2F). This was reflected in the composition of bile acids in the gallbladder. Although the total bile acid content did not differ, *Lrh-1 K289R* mice had slightly increased tauro-conjugated cholic acid (tCA) and less tauro-conjugated muricholic acid (tMCA) (Figure S2C). Altogether, these data show that LRH-1 K289R exhibits increased transcriptional activity on a selected subset of LRH-1 target genes and cannot be described as a global constitutive active LRH-1 form.

LRH-1 K289R Protects against Atherosclerosis Development

Given that many of the genes affected in *Lrh-1 K289R* mice are involved in cholesterol homeostasis, we hypothesized that LRH-1 K289R may affect cholesterol metabolism, and hence hypercholesterolemia-driven diseases, such as atherosclerosis. To study the role of LRH-1 K289R in atherosclerosis, we crossbred *Lrh-1 WT* and *Lrh-1 K289R* mice to atherosclerotic-prone *Ldlr* knockout mice in order to generate *Ldlr*$^{-/-}$ *Lrh-1 WT* (LL-WT) or *Ldlr*$^{-/-}$ *Lrh-1 K289R* (LL-K289R) mice. Then, 8-week-old LL-WT or LL-K289R mice were subjected to a high-cholesterol diet (HCD) for 14 weeks. Body and liver weight (Figures S3A and S3B), and also gross morphology of other organs, were similar between the different genotypes (data not shown). Notably, en face plaque analyses of the thoraco-abdominal aorta demonstrated that LL-K289R mice developed significantly less atherosclerotic plaques than LL-WT mice and also accumulated less cholesterol in their aortas (Figures 3A–3C). Advanced plaque analyses of the aortic sinus stained for collagen imaging revealed no changes in necrotic core size, cap thickness, or collagen content in LL-K289R in comparison to LL-WT mice (Figures S3C–S3E). Total plasma cholesterol did not differ between the mice, and plasma triglyceride levels were only slightly reduced before administering the HCD and were not significantly changed upon HCD feeding (Figures S3F and S3G). Although no changes in triglyceride content were observed in the lipoprotein fractions, a small reduction in the cholesterol content of the low-density lipoprotein subfraction of LL-K289R mice could be noticed (Figures S3H and S3I). Furthermore, hepatic triglyceride content was not changed in overnight fasted LL-K289R mice, whereas cholesterol content was only slightly increased (Figure 3D). Stainings of liver cryosections showed no apparent difference in neutral lipid content and cellular morphology between the two genotypes (Figure 3E). These data demonstrate that LL-K289R mice develop less atherosclerosis, possibly as a consequence of improved RCT.

To assess a potential contribution of macrophages in the observed phenotype, we measured *Lrh-1* in isolated thioglycolate-elicited peritoneal macrophages. In comparison to its expression in the liver, *Lrh-1* was barely detectable in macrophages under the conditions analyzed (Figure S4A; bioGPS *Lrh-1* expression pattern, http://biogps.org/#goto=genereport&id=26424). Furthermore, treatment with acetylated LDL (acLDL) to trigger

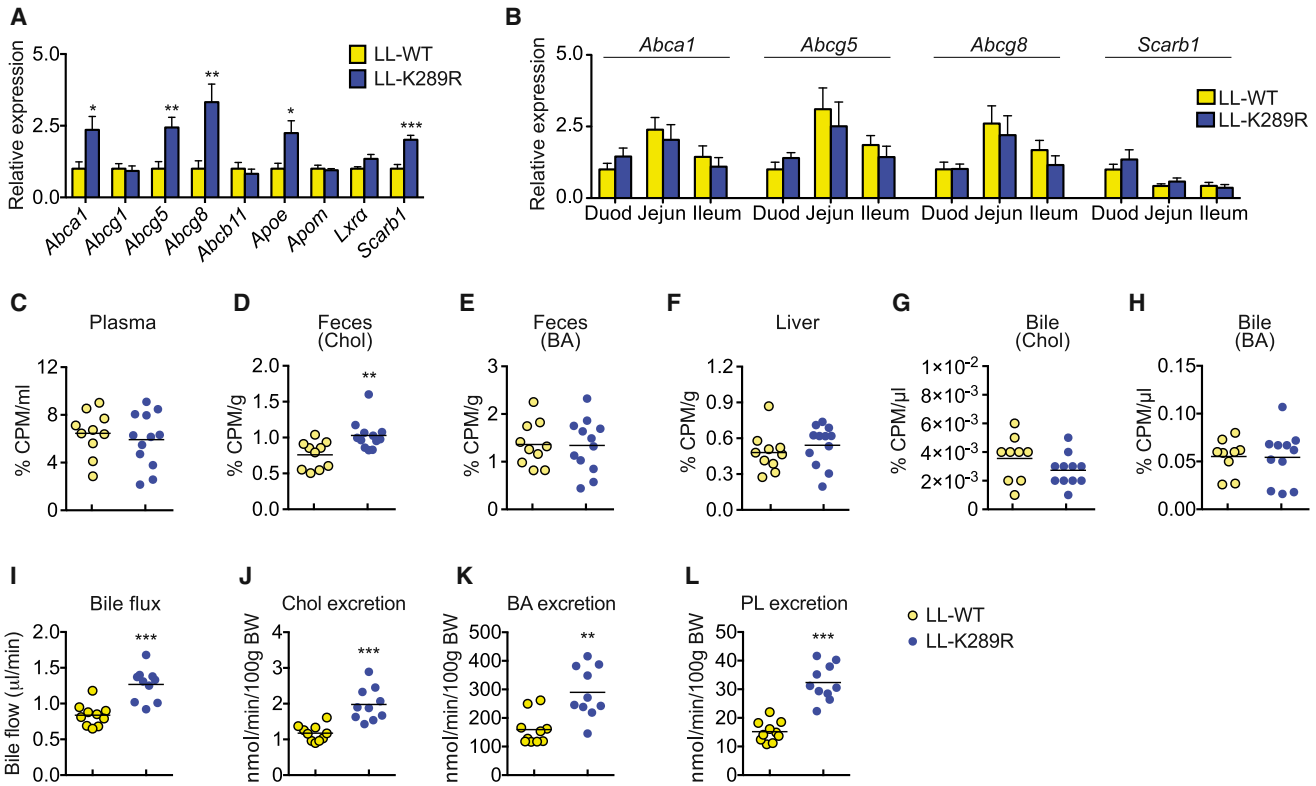

Figure 4. Improved Reverse Cholesterol Transport and Biliary Sterol Excretion in LL-K289R Mice

(A) Hepatic expression of genes affecting cholesterol metabolism in LL-WT and LL-K289R mice. n = 9 per genotype.

(B) Intestinal expression of genes affecting cholesterol metabolism in LL-WT and LL-K289R mice. Duod, duodenum; Jejun, jejunum. n = 9 per genotype.

(C–H) LL-WT and LL-K289R mice were injected with ^{3}H-cholesterol loaded LL-WT macrophages. Detection of ^{3}H-tracer in plasma (C), fecal cholesterol (Chol; D), fecal bile acids (BA; E), liver (F), bile cholesterol fraction (G), and bile BA fraction (H). n = 10 LL-WT; n = 12 LL-K289R.

(I–L) Bile excretion (I) and biliary secretion rates of Chol (J), BA (K), and phospholipids (PL; L). n = 10 per genotype.

Data are represented as means ± SEM. *p < 0.05, **p < 0.01, ***p < 0.001 relative to LL-WT, as determined by Mann-Whitney U or Student's t tests. See also Figure S4.

foam cell formation or lipopolysaccharide (LPS) in order to evaluate the inflammatory response did not trigger any significant difference in acetylated LDL accumulation, *Scarb1* expression, or inflammatory markers between *Lrh-1 WT* and *K289R* macrophages (Figures S4B–S4H), suggesting that the effects on aortic lipid accumulation are not likely related to differential macrophage function.

LRH-1 K289R Protects against Atherosclerosis by Promoting RCT

Intrigued by the marked decrease of atherosclerotic lesions in LL-K289R mice and the increased expression of genes involved in hepatic cholesterol homeostasis in *Lrh-1 K289R* mice (Figure 2F), we analyzed the expression of genes involved in RCT in the liver. Notably, hepatic expression of *Abca1*, *Abcg5*, *Abcg8*, *Apoe*, and *Scarb1* was significantly increased in LL-K289R in comparison to LL-WT mice (Figure 4A). Given that many of these genes are also expressed in the intestine and contribute to whole-body cholesterol homeostasis, we analyzed their expression pattern in the duodenum, jejunum, and ileum. Surprisingly, none of these transcripts was increased in any of the three intestinal sections (Figure 4B). Moreover, microarray analyses of jejunal sections from *Lrh-1 K289R* and *Lrh-1 WT* mice did not display differential expression of cholesterol and lipoprotein regulators that are expressed in livers and intestine (Figure S4I), indicating that LRH-1 K289R specifically induces the expression of cholesterol transport regulators in the liver.

To analyze whether the increased expression of RCT genes has physiological consequences, we performed in vivo macrophage-to-feces RCT and biliary flux studies. In vivo RCT analysis was performed by injecting peritoneal macrophages that were loaded with [^{3}H]-cholesterol (^{3}H tracer) ex vivo into recipient LL-K289R and LL-WT mice. ^{3}H-tracer counts were significantly increased in the fecal cholesterol fraction of LL-K289R in comparison to LL-WT mice, whereas no major differences were observed in the fecal bile acid pool or the plasma, hepatic, or biliary pools (Figures 4C–4H). Furthermore, gallbladder cannulation revealed that bile flow was increased in LL-K289R in comparison to LL-WT mice (Figure 4I). In line with the increased bile flow, biliary cholesterol, bile acids, and phospholipids excretion were also enhanced in LL-K289R in comparison to LL-WT mice (Figures 4J–4L). These data establish LRH-1 K289R as a potent mediator of bile secretion and RCT in vivo.

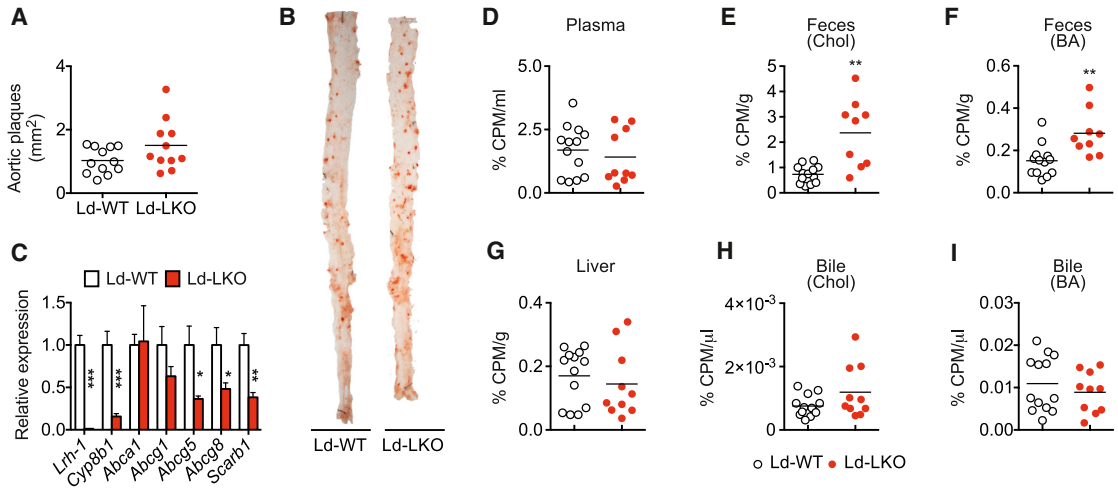

Figure 5. Liver-Specific *Lrh-1* Knockout Mice Do Not Develop More Atherosclerosis

(A) Quantification of aortic plaque area in $Ldlr^{-/-}$ $Lrh\text{-}1^{hep+/+}$ (Ld-WT, n = 12) or $Ldlr^{-/-}$ $Lrh\text{-}1^{hep-/-}$ (Ld-LKO, n = 11) mice.

(B) Representative aortas of Ld-WT and Ld-LKO mice stained with Oil-Red O.

(C) Hepatic expression of genes affecting cholesterol metabolism in Ld-WT and Ld-LKO mice. n = 9 per genotype.

(D–I) Ld-WT and Ld-LKO mice were injected with ^{3}H-cholesterol loaded Ld-WT macrophages. Detection of ^{3}H tracer in plasma (D), fecal cholesterol (E), fecal BA (F), liver (G), bile Chol fraction (H), and bile BA fraction (I). n = 13 Ld-WT; n = 10 Ld-LKO.

Data are represented as means ± SEM. *p < 0.05, **p < 0.01, ***p < 0.001 relative to LL-WT, as determined by Student's t test. See also Figure S5.

Liver-Specific *Lrh-1* Knockout Mice Do Not Develop Increased Atherosclerosis

Even though the transcriptome and targeted gene expression analyses argue against Lrh-1 K289R as a simple constitutively active form of LRH-1 (Figures 2D–2F), we nevertheless explored whether the hepatocyte-specific $Lrh\text{-}1^{hep-/-}$ mice would yield an opposite phenotype on RCT and atherosclerosis development. Therefore, we crossbred hepatocyte-specific $Lrh\text{-}1^{hep-/-}$ with $Ldlr^{-/-}$ mice in order to generate $Ldlr^{-/-}$ $Lrh\text{-}1^{hep+/+}$ (Ld-WT) or $Ldlr^{-/-}$ $Lrh\text{-}1^{hep-/-}$ (Ld-LKO) mice and fed them an HCD for 12 weeks. Body and liver weight did not differ between the genotypes (Figures S5A and S5B). Interestingly, Ld-LKO did not develop more atherosclerotic lesions than Ld-WT mice (Figures 5A and 5B), although the expression of the RCT regulators (Figure 5C) and binding of LRH-1 to the *Abcg5/Abcg8* intergenic promoter (Freeman et al., 2004) (Figure S5C) was significantly lower in the Ld-LKO liver. Moreover, in vivo RCT analysis demonstrated an increased fecal sterol content in Ld-LKO mice, which could explain why these mice do not develop more atherosclerotic lesions (Figures 5D–5I). The increase of fecal sterols in $Lrh\text{-}1^{hep-/-}$ mice most likely stems from the compromised intestinal sterol absorption, which was previously reported to be the consequence of reduced *Cyp8b1* in the liver shifting the bile acid pool toward more hydrophilic bile acids (Figure 5C) (Mataki et al., 2007; Out et al., 2011).

Compromised Binding of LRH-1 K289R with the Corepressor PROX1 Derepresses Hepatic RCT Genes

Several corepressors have been reported to fine-tune the activity of LRH-1 in a context specific manner. In the liver, corepressors such as small heterodimer partner (SHP or NR0B2) and prospero homeobox protein 1 (PROX1) as well as the NCOR1/HDAC3 corepressor complex can repress LRH-1 activity (Goodwin et al., 2000; Lee and Moore, 2002; Lu et al., 2000; Qin et al., 2004; Venteclef et al., 2010). To test the assumption that LRH-1 SUMOylation affects the interaction of LRH-1 with potential corepressors, we carried out coimmunoprecipitation experiments in HEK293T cells transfected with LRH-1 WT or LRH-1 K289R in the presence of the corepressor SHP, PROX1, or NCOR1. Surprisingly, we observed that the interaction between LRH-1 and PROX1 was lost or much weaker when LRH-1 K289R was ectopically expressed (Figure 6A), whereas no difference in interaction was observed with SHP or detected with NCOR1 (data not shown). This would suggest that optimal PROX1-LRH-1 interaction may at least require transient SUMOylation of K289 of LRH-1 WT. To assess this possibility, we coexpressed the isopeptidase SENP1 in order to enzymatically remove SUMO from its substrates. SENP1 robustly reduced the interaction between LRH-1 WT and PROX1, supporting the hypothesis that the SUMOylation status affects the interaction (Figure 6B), which might be direct or be mediated by a third partner. Interestingly, the weaker interaction observed between PROX1 and LRH-1 K289R was further reduced by addition of SENP1, suggesting that other SUMOylatable sites in the protein complex may enhance the interaction between the two proteins (Figure 6B). Given that loss of binding to the corepressor PROX1 would provide a mechanistic basis for explaining the enhanced activity of LRH-1 K289R, we next explored whether differential *Prox1* expression between liver and intestine could explain the absence of effects on intestinal RCT genes in *Lrh-1 K289R* mice (Figure 4B). Interestingly, *Prox1* mRNA was almost undetectable in the small intestine and only marginally expressed in the colon in comparison to liver (Figure 6C; bioGPS *Prox1* expression pattern, http://biogps.org/#goto=genereport&id=26424), thus most likely contributing to the differential expression of RCT genes between liver and intestine.

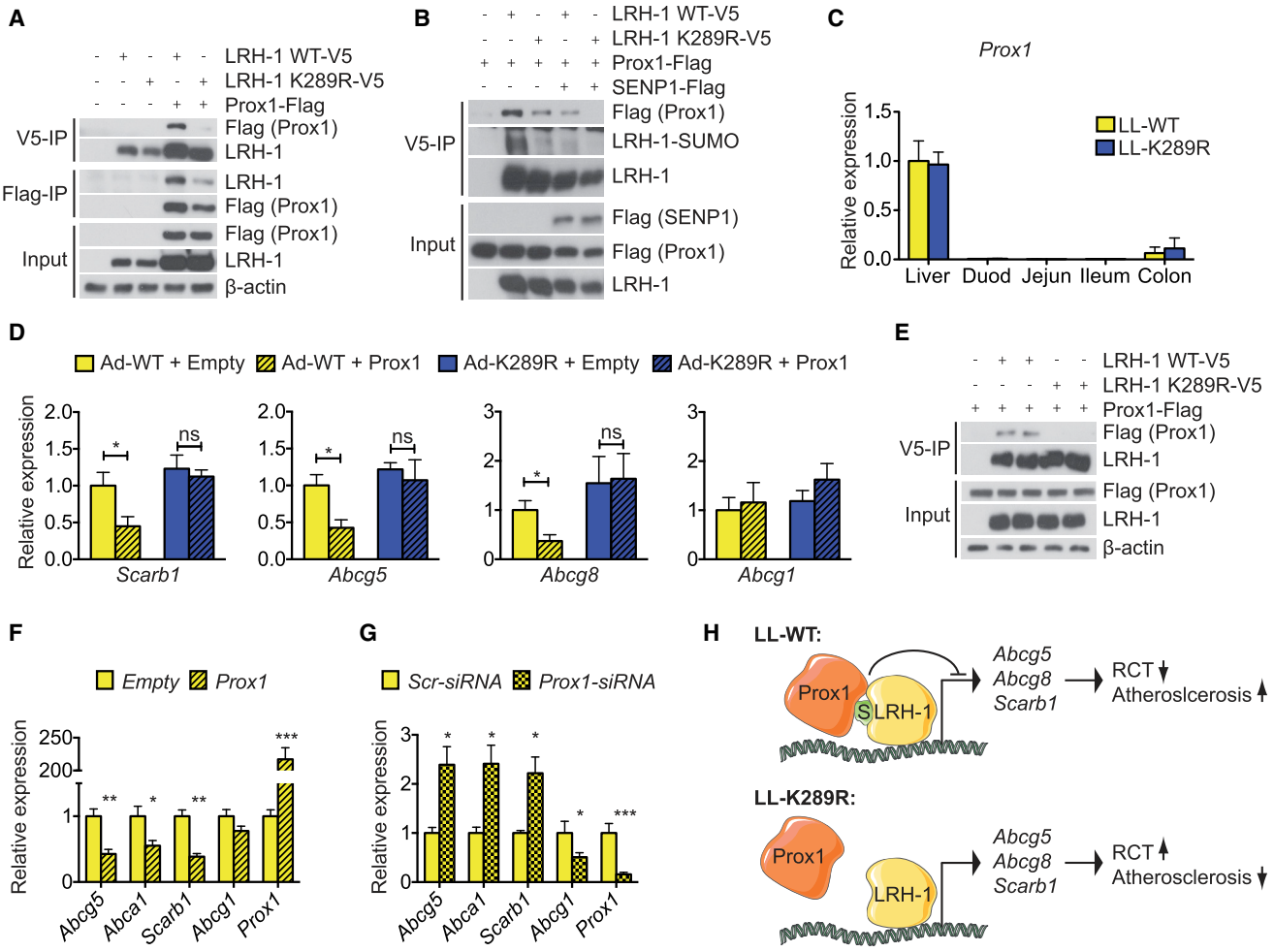

Figure 6. Compromised Binding of LRH-1 K289R with Prox1 Derepresses Hepatic RCT Genes

(A) LRH-1/Prox1 CoIP in HEK293T cells overexpressing V5-tagged LRH-1 (WT or K289R) and FLAG-tagged Prox1. The experiment was replicated at least three times.

(B) LRH-1/Prox1 CoIP in HEK293T cells overexpressing V5-tagged LRH-1 (WT or K289R), FLAG-tagged Prox1, and FLAG-tagged SENP1. The experiment was replicated three times.

(C) Comparative *Prox1* expression in liver, duodenum (Duod), jejunum (Jejun), ileum, and colon of LL-WT and LL-K289R mice. n = 9 per genotype.

(D) Expression of *Scarb1*, *Abcg5*, *Abcg8*, *Abca1*, and *Abcg1* in *Lrh-1*$^{hep-/-}$ primary hepatocytes that were infected or transfected with LRH-1 (WT or K289R) and Prox1. n = 3. The experiment was replicated with three batches of primary cells.

(E) LRH-1/Prox1 CoIP in primary hepatocytes that were infected or transfected with V5-tagged LRH-1 (WT or K289R) and FLAG-tagged Prox1. n = 2 from independent batches of primary hepatocytes.

(F and G) Effect of overexpression (F) and small-interfering-RNA-mediated silencing (G) of *Prox1* in WT primary hepatocytes n = 3. The experiment was replicated with two batches of primary cells.

(H) Model showing how LRH-1 WT and LRH-1 K289R regulate the expression of key genes controlling hepatic cholesterol transport and its consequence on RCT and atherosclerosis. S, SUMO-1.

Data are represented as means ± SEM. *p < 0.05 and **p < 0.01 relative to non-*Prox-1*-transfected controls, as determined by Student's t test. See also Figure S6.

To study the molecular effect of the PROX1-LRH-1 interaction in more detail, we decided to use primary hepatocytes. Notably, both *Lrh-1* and *Prox1* transcripts were reduced to ~25% of their expression in whole livers but were clearly detectable (Figure S6A). We isolated primary hepatocytes from *Lrh-1*$^{hep-/-}$ mice and infected them with an adenovirus containing the LRH-1 WT or K289R followed by ectopic expression of PROX1. Interestingly, while expression of *Abcg1* was not affected or rather increased in cells overexpressing PROX1, the expression of *Scarb1*, *Abcg5*, and *Abcg8* was diminished in cells in which LRH-1 WT, but not LRH-1 K289R, was reconstituted (Figures 6D and S6B), demonstrating that the repressive function of PROX1 on LRH-1 activity depends on an intact LRH-1 K289 SUMOylation site. Furthermore, LRH-1 K289R failed to bind PROX1 in transfected primary hepatocytes, whereas LRH-1 WT/PROX1 interaction was intact (Figure 6E), demonstrating that the LRH-1/PROX1 complex can assemble in vitro and ex vivo. To assess whether we could mimic the effect

of LRH-1/PROX1 interaction in a physiologically relevant cell model, we next overexpressed or silenced *Prox1* in WT primary hepatocytes. While overexpression of *Prox1* reduced the expression of the RCT regulators (Figure 6F), silencing of *Prox1* had the opposite effect (Figure 6G). Altogether, our data suggest that SUMOylated LRH-1 WT recruits the corepressor PROX1 and hence is unable to selectively activate the transcription of important cholesterol receptors and transporters (Figure 6H). If SUMOylation of LRH-1 is defective as in our LRH-1 K289R mutant, then the PROX1-mediated repression is weakened or lost, thereby facilitating the induction of RCT genes and diminishing the progression of atherosclerosis (Figure 6H).

DISCUSSION

Posttranslational modification by SUMO affects the function of a large number of nuclear proteins, including NRs (Geiss-Friedlander and Melchior, 2007; Treuter and Venteclef, 2011). Although various NRs have emerged as reversible SUMO targets modulating almost every aspect of NR function in cell models, very few studies have established in vivo functional roles of NR SUMOylation in health or disease. This is rather surprising given the prominent role of NRs in the pathogenesis of diseases and the repressive imprint of SUMOylation on NR activity. In this study, we have generated a mouse model harboring a K289R mutation that strongly affects LRH-1 SUMOylation and function. We demonstrate that loss of SUMOylation by mutating the critical lysine acceptor site in the LRH-1 protein is sufficient to protect mice against the development of a chronic metabolic disease such as atherosclerosis. More importantly, we provide evidence that the beneficial effect on atherosclerosis is caused by enhancing the transcription of hepatic RCT genes, such as *Abca1*, *Abcg5*, *Abcg8*, and *Scarb1*, without any involvement of gut- or macrophage-specific RCT genes. These findings are consistent with a recent study in *Drosophila* showing that SUMOylation of the LRH-1 homolog *Ftz-f1* affects the expression of the scavenger receptor *Snmp1*, which is required for cellular cholesterol uptake and subsequent steroid synthesis (Talamillo et al., 2013), suggesting that LRH-1 SUMOylation may impact on a similar physiologically conserved pathway.

Alignment of the protein sequence of LRH-1 with other NRs revealed that, aside from SF-1, only members of the ROR family have a hinge region that is comparable to that of LRH-1 (Figure 2B). Although in SF-1, mutation of two conserved SUMO acceptor lysine residues in the hinge region leads to a striking developmental phenotype in mice, characterized by inappropriate sonic hedgehog signaling and impaired endocrine tissue development (Lee et al., 2011a), our study shows that disruption of only one of these conserved SUMO sites in LRH-1 has a significant impact on adult homeostasis and protects against the development of a chronic disease. Surprisingly, SUMOylation of the homologous motif in RORα seems to activate instead of repressing its transcriptional activity (Hwang et al., 2009); however, its physiological properties have not been reported. These studies collectively indicate that SUMOylation of the hinge region has profound functional consequences among a very small subset of NRs.

The mechanistic features by which SUMO modulates the activity of NRs vary considerably and can range from interference with- to promotion of protein-protein interactions or alternatively competition with other PTMs (Geiss-Friedlander and Melchior, 2007; Jentsch and Psakhye, 2013). Our data suggest a role for LRH-1 SUMOylation in promoting protein-protein interactions. This finding is in line with previous studies showing that SUMOylation of LRH-1 K224, the human lysine residue corresponding to mouse LRH-1 K289, binds to a transcriptional corepressor complex consisting of NCOR1, HDAC3, and GPS2 and regulates the expression of acute phase response genes in human hepatoma cells (Venteclef et al., 2010). Interestingly, this study further demonstrated that mouse LRH-1 binding to the *haptoglobin* promoter was reduced in *Sumo1* knockout in comparison to WT livers. In our study, we reveal an unanticipated mechanism by demonstrating that LRH-1 K289R fails to bind another corepressor (i.e., PROX1), and we furthermore show that this impacts on the RCT genes, ultimately leading to enhanced bile flow and atheroprotection. The study by Venteclef et al. (2010), along with our work, propose that SUMOylation of a single K residue of LRH-1 promotes the recruitment of specific corepressor complexes. Importantly, our data demonstrate that the effect of LRH-1 SUMOylation depends on tissue-specific corepressor interaction.

The physiological stimuli and timing that affect LRH-1 SUMOylation in the liver are unknown. In primary granulosa cells, SUMO-driven sequestration of LRH-1 into nuclear bodies is abruptly reversed by cAMP and results in the induction of LRH-1 target genes (Yang et al., 2009). Intriguingly, this is accompanied by a robust reduction of the *Ubc9* and *Pias3* genes, which are part of the SUMO conjugation machinery. Conversely, expression of the SUMO-specific isopeptidase *Senp2* was increased. Although the crosstalk with the cAMP signaling has not been evaluated in the context of LRH-1 SUMOylation in liver cells, it is tempting to speculate that different physiological and/or pharmacological cues could trigger specific posttranslational modifications in LRH-1, which in turn could recruit specific corepressor complexes.

Several studies have identified natural or synthetic LRH-1 activators and inhibitors (Ingraham and Redinbo, 2005). A recent study has identified the unusual phospholipid dilauroyl phosphatidylcholine as an LRH-1 ligand (Lee et al., 2011b). Future studies should test whether ligand activation, posttranslational modifications such as SUMOylation, and coregulator recruitment are interconnected. The tissue and context-specific nature of such effects may offer an ideal therapeutic window for activating a receptor and exploit beneficial effects, without causing adverse effects that are common with NR therapeutics (Marciano et al., 2014). In this context, it is important to point out that the biological effects of LRH-1 K289R cannot be compared to those induced by a gain-of-function of LRH-1 or by a potential drug that would enhance the activity of LRH-1 in a broader manner. In fact, the *Lrh-1 K289R* mice show increased activation of selected LRH-1 target genes, whereas other targets are not affected. The *Lrh-1 K289R* mice also seem to display no effects on RCT in the gut, most likely because LRH-1 and PROX-1 are not coexpressed in the same cells of the crypt-villus epithelium (Botrugno et al., 2004) or because of the low abundance of PROX-1 in the intestinal mucosa (Figure 6C). Likewise, no changes on *Scarb1* gene expression could be detected in macrophages (Figure S4E). Such a restriction of the effects of LRH-1

to selected tissues—in this case, the liver—and a subset of target genes, may be the key to drive only antiatherogenic effects of LRH-1. A better understanding into how SUMOylation of LRH-1 and ensuing coregulator recruitment can be modulated will be instrumental and may provide opportunities for pharmacological intervention to combat common diseases, such as atherosclerosis.

EXPERIMENTAL PROCEDURES

Animal Studies

The generation of the *Lrh-1 K289R* mouse model is described in detail in the Supplemental Experimental Procedures. Congenic C57Bl/6J *Lrh-1 WT* or *Lrh-1 K289R* mice were crossbred with congenic C57Bl/6J *Ldlr* knockout mice in order to generate $Ldlr^{-/-}$ *Lrh-1 WT* (LL-WT) or $Ldlr^{-/-}$ *Lrh-1 K289R* (LL-K289R) mice. LL-WT and LL-K289R mice were kept on an HCD (1.25% total cholesterol, Harlan TD.94059) for 14 weeks starting at the age of 8 weeks. Similarly, congenic C57Bl/6J $Lrh\text{-}1^{hep-/-}$ and $Lrh\text{-}1^{hep+/+}$ mice (Oosterveer et al., 2012) were crossbred with $Ldlr^{-/-}$ mice in order to generate $Ldlr^{-/-}$ $Lrh\text{-}1^{hep+/+}$ (Ld-WT) or $Ldlr^{-/-}$ $Lrh\text{-}1^{hep-/-}$ (Ld-LKO) mice and fed a HCD for 12 weeks. All animal procedures were approved by the Swiss authorities (Canton of Vaud, animal protocols ID #2561 and #2768) and performed in accordance with our institutional guidelines.

Site-directed mutagenesis, subcellular fractionation of liver tissue, immunoprecipitation (IP), Coimmunoprecipitation (CoIP), and western blotting are explained in the Supplemental Experimental Procedures.

Protein Alignment

All protein alignments were performed with the standard Geneious (Blosum62 matrix) or ClustalW (BLOSUM matrix) algorithm from the Geneious software (http://www.geneious.com).

Gene Expression and Analysis

RNA was extracted from the livers and jejunums of ad libitum fed Lrh-1 WT (n = 7) and Lrh-1 K289R (n = 7) mice and from liver of ad libitum fed Lrh-$1hep^{+/+}$ (n = 8) and Lrh-$1hep^{-/-}$ (n = 8) mice with TRIZOL (Invitrogen) and purified with the RNeasy Cleanup Kit for Microarray Analysis (QIAGEN). For quantitative RT-PCR (qRT-PCR), cDNA was generated with the QuantiTect Reverse Transcription Kit (QIAGEN) and analyzed by qPCR with a LightCycler 480 Real-Time PCR System (Roche), and the primers are listed in the Table S2. Expression data were normalized to *36B4* or *B2M* mRNA levels. Microarray analysis was performed with the Affymetrix MouseGene 1.0 ST or Affymetrix MouseGene 2.0 ST array and normalized with the robust multiarray average method. A table of reciprocally regulated transcripts is provided in Table S1. Venn diagram analysis and heatmaps were performed with GENE-E (http://www.broadinstitute.org/cancer/software/GENE-E/index.html). For the Venn diagram, the overlap of nominally significantly changed genes ($p < 0.05$ and fold change ≥ 1.5) among the groups was analyzed.

Chromatin Immunoprecipitation

ChIP analysis was performed as described previously with minor modifications (Duggavathi et al., 2008). DNA was purified with the PCR Clean-up extraction kit (Macherey-Nagel), after which qPCR was performed as described previously (Mataki et al., 2007). Data were normalized to the input (fold differences = $2^{-(Ct\ sample\ -\ Ct\ input)}$). ChIP primer sequences are listed in Table S3.

Lipoprotein Separation

Pooled plasma samples were subjected to fast protein liquid chromatography gel filtration with a Superose 6 Column (GE Healthcare). Individual fractions were assayed for cholesterol and triglyceride concentrations with commercially available enzymatic assays (Roche).

Hepatic Lipid Analyses

Hepatic lipids were extracted according to the Bligh and Dyer (1959) protocol. Triglyceride and cholesterol contents in plasma and hepatic lipid fractions were quantified with enzymatic assays (Roche).

Cholesterol Uptake and LPS Stimulation of Peritoneal Macrophages

Thioglycolate-elicited peritoneal macrophages were harvested, cultured, and starved in vitro and then loaded with 50 μg/ml Dil-labeled acetylated LDL for 4 hr in order to assess the cholesterol uptake or 10 ng/ml LPS for 4 hr in order to analyze the expression of inflammatory markers.

Reverse Cholesterol Transport

RCT protocol was adapted from Meissner et al. (2010). In brief, thioglycolate-elicited mouse peritoneal macrophages were harvested, cultured in vitro, loaded with 50 μg/ml acetylated LDL and 3 μCi/ml 3H-cholesterol for 24 hr, and equilibrated in RPMI 1640 medium containing 1% penicillin/streptomycin and 0.2% BSA for 6 hr. For in vivo RCT, two million labeled LL-WT macrophages were injected intraperitoneally into recipient LL-WT or LL-K289R mice. Mice were sacrificed 48 hr postinjection, and plasma, liver, gallbladder, and feces were stored at −80°C until further analysis. Counts within liver were determined after the solubilization of the tissue. Fecal samples were dried, weighed, and thoroughly ground. Then, aliquots were separated into bile acid and neutral sterol fractions prior to liquid scintillation counting.

Bile Flow and Bile Composition

Bile duct cannulation was performed as described previously (Kruit et al., 2005) with LL-WT and LL-K289R mice. In brief, hepatic bile was collected for 30 min from the common bile duct via cannulation of the gallbladder, and bile flow was determined gravimetrically assuming a density of 1 g/ml for bile. Bile composition was analyzed by high performance liquid chromatography (HPLC) tandem mass spectrometry as described previously (Mataki et al., 2007).

Primary Cell Culture

Primary hepatocytes from hepatocyte-specific $Lrh\text{-}1^{hep-/-}$ mice were isolated with Liberase Blendzyme (Roche) perfusion as described previously with minor modifications (Ryu et al., 2011). $Lrh\text{-}1^{hep-/-}$ hepatocytes were plated in Dulbecco's modified Eagle's medium 4.5 g/l glucose with 10% fetal bovine serum. Cells were infected with an adenovirus expressing LRH-1 WT or LRH-1 K289R 4 hr after plating followed by transfection of a Prox1 plasmid with Lipofectamine 2000 (Invitrogen). Cells were lysed 48 hr postinfection and used for subsequent analysis.

Reporter Assays

Transient transfections in HEK293T cells were performed with Lipofectamine 2000 (Invitrogen) or JetPEI (Polyplus) as previously described (Oosterveer et al., 2012). In brief, cells were transfected with pTK-GL3 reporter constructs driven by a heterologous promoter consisting of multiple consensus LRH-1 response elements (pGL3::$(LRHRE)_5$-TK-LUC) in the presence of either pCMX::LRH-1 WT or the KR mutant constructs. Luciferase activities were measured 24 hr posttransfection and normalized to β-galactosidase activities.

Immunohistochemistry

En face plaque analysis was performed on thoraco-abdominal aortae that were fixed with 10% paraformaldehyde overnight and then stained with Oil-Red O (Stein et al., 2010). Aortic sinuses were cut into 5-μm-thick serial cryosections and stained with Sirius Red in order to measure necrotic core size, cap thickness, and collagen content (Stein et al., 2010). Means were taken from n = 6 mice per genotype, and three serial cryosections were evaluated from each mouse.

Statistical Analyses

Data are expressed as means ± SEM. Analysis of en face atherosclerotic plaque content and bile excretion rates was carried out with Mann-Whitney U tests. Comparison of differences between two groups of other experiments was assessed with unpaired two-tailed Student's t tests. Multiple group comparisons were assessed by one-way ANOVA and Bonferonni post hoc tests. $p < 0.05$ was considered statistically significant (*$p < 0.05$, **$p < 0.01$, ***$p < 0.001$).

ACCESSION NUMBERS

All microarray data are accessible at the NCBI Gene Expression Omnibus under number GSE59333.

SUPPLEMENTAL INFORMATION

Supplemental Information contains Supplemental Experimental Procedures, six figures, and three tables and can be found with this article online at http://dx.doi.org/10.1016/j.cmet.2014.07.023.

AUTHOR CONTRIBUTIONS

S.S. carried out most of the experiments, data analysis, and prepared the figures and the manuscript. M.H.O. and R.H. performed lipoprotein analysis and the bile cannulation experiment. C.M. made the initial mutant LRH-1 constructs and carried out reporter assays. P.X. helped with qPCR, stainings, and CoIP experiments. V.L. and A.P. helped with lipid extractions and macrophage isolation. D.R. assisted with the generation of adenoviral constructs. K.J.M. helped with the isolation of primary hepatocytes. X.W. helped with microarray and bioinformatic analyses. C.D. and F.M. helped with SUMOylation assays. S.M.H. performed HPLC analysis of the bile. K.S. designed the experiments and supervised all aspects of the work.

ACKNOWLEDGMENTS

We thank S. Bichet, N. Moullan, and T. Clerc for technical help and Xavier Warot and the Institut Clinique de la Souris for the generation of the LRH-1 K289R mouse. The pcDNA3.1-FLAG::Prox1 plasmid was kindly provided by Panagiotis Politis. This study was supported by EPFL funding and grants from the Swiss Heart Foundation and the Swiss Cancer League (KLS-2809-08-2011). S.S. is supported by a postdoctoral fellowship from the German Academy of Sciences Leopoldina (LPDS 2011-6).

Received: March 4, 2014
Revised: June 12, 2014
Accepted: July 24, 2014
Published: August 28, 2014

REFERENCES

Bernier-Villamor, V., Sampson, D.A., Matunis, M.J., and Lima, C.D. (2002). Structural basis for E2-mediated SUMO conjugation revealed by a complex between ubiquitin-conjugating enzyme Ubc9 and RanGAP1. Cell *108*, 345–356.

Bligh, E.G., and Dyer, W.J. (1959). A rapid method of total lipid extraction and purification. Can. J. Biochem. Physiol. *37*, 911–917.

Botrugno, O.A., Fayard, E., Annicotte, J.S., Haby, C., Brennan, T., Wendling, O., Tanaka, T., Kodama, T., Thomas, W., Auwerx, J., and Schoonjans, K. (2004). Synergy between LRH-1 and beta-catenin induces G1 cyclin-mediated cell proliferation. Mol. Cell *15*, 499–509.

Chalkiadaki, A., and Talianidis, I. (2005). SUMO-dependent compartmentalization in promyelocytic leukemia protein nuclear bodies prevents the access of LRH-1 to chromatin. Mol. Cell. Biol. *25*, 5095–5105.

Coste, A., Dubuquoy, L., Barnouin, R., Annicotte, J.S., Magnier, B., Notti, M., Corazza, N., Antal, M.C., Metzger, D., Desreumaux, P., et al. (2007). LRH-1-mediated glucocorticoid synthesis in enterocytes protects against inflammatory bowel disease. Proc. Natl. Acad. Sci. USA *104*, 13098–13103.

Duggavathi, R., Volle, D.H., Mataki, C., Antal, M.C., Messaddeq, N., Auwerx, J., Murphy, B.D., and Schoonjans, K. (2008). Liver receptor homolog 1 is essential for ovulation. Genes Dev. *22*, 1871–1876.

Fayard, E., Schoonjans, K., Annicotte, J.S., and Auwerx, J. (2003). Liver receptor homolog 1 controls the expression of carboxyl ester lipase. J. Biol. Chem. *278*, 35725–35731.

Fayard, E., Auwerx, J., and Schoonjans, K. (2004). LRH-1: an orphan nuclear receptor involved in development, metabolism and steroidogenesis. Trends Cell Biol. *14*, 250–260.

Fernandez-Marcos, P.J., Auwerx, J., and Schoonjans, K. (2011). Emerging actions of the nuclear receptor LRH-1 in the gut. Biochim. Biophys. Acta *1812*, 947–955.

Freeman, L.A., Kennedy, A., Wu, J., Bark, S., Remaley, A.T., Santamarina-Fojo, S., and Brewer, H.B., Jr. (2004). The orphan nuclear receptor LRH-1 activates the ABCG5/ABCG8 intergenic promoter. J. Lipid Res. *45*, 1197–1206.

Geiss-Friedlander, R., and Melchior, F. (2007). Concepts in sumoylation: a decade on. Nat. Rev. Mol. Cell Biol. *8*, 947–956.

Goodwin, B., Jones, S.A., Price, R.R., Watson, M.A., McKee, D.D., Moore, L.B., Galardi, C., Wilson, J.G., Lewis, M.C., Roth, M.E., et al. (2000). A regulatory cascade of the nuclear receptors FXR, SHP-1, and LRH-1 represses bile acid biosynthesis. Mol. Cell *6*, 517–526.

Hwang, E.J., Lee, J.M., Jeong, J., Park, J.H., Yang, Y., Lim, J.S., Kim, J.H., Baek, S.H., and Kim, K.I. (2009). SUMOylation of RORalpha potentiates transcriptional activation function. Biochem. Biophys. Res. Commun. *378*, 513–517.

Ingraham, H.A., and Redinbo, M.R. (2005). Orphan nuclear receptors adopted by crystallography. Curr. Opin. Struct. Biol. *15*, 708–715.

Jentsch, S., and Psakhye, I. (2013). Control of nuclear activities by substrate-selective and protein-group SUMOylation. Annu. Rev. Genet. *47*, 167–186.

Krasowski, M.D., Reschly, E.J., and Ekins, S. (2008). Intrinsic disorder in nuclear hormone receptors. J. Proteome Res. *7*, 4359–4372.

Kruit, J.K., Plösch, T., Havinga, R., Boverhof, R., Groot, P.H., Groen, A.K., and Kuipers, F. (2005). Increased fecal neutral sterol loss upon liver X receptor activation is independent of biliary sterol secretion in mice. Gastroenterology *128*, 147–156.

Lee, Y.K., and Moore, D.D. (2002). Dual mechanisms for repression of the monomeric orphan receptor liver receptor homologous protein-1 by the orphan small heterodimer partner. J. Biol. Chem. *277*, 2463–2467.

Lee, Y.K., and Moore, D.D. (2008). Liver receptor homolog-1, an emerging metabolic modulator. Front. Biosci. *13*, 5950–5958.

Lee, M.B., Lebedeva, L.A., Suzawa, M., Wadekar, S.A., Desclozeaux, M., and Ingraham, H.A. (2005). The DEAD-box protein DP103 (Ddx20 or Gemin-3) represses orphan nuclear receptor activity via SUMO modification. Mol. Cell. Biol. *25*, 1879–1890.

Lee, F.Y., Faivre, E.J., Suzawa, M., Lontok, E., Ebert, D., Cai, F., Belsham, D.D., and Ingraham, H.A. (2011a). Eliminating SF-1 (NR5A1) sumoylation in vivo results in ectopic hedgehog signaling and disruption of endocrine development. Dev. Cell *21*, 315–327.

Lee, J.M., Lee, Y.K., Mamrosh, J.L., Busby, S.A., Griffin, P.R., Pathak, M.C., Ortlund, E.A., and Moore, D.D. (2011b). A nuclear-receptor-dependent phosphatidylcholine pathway with antidiabetic effects. Nature *474*, 506–510.

Lu, T.T., Makishima, M., Repa, J.J., Schoonjans, K., Kerr, T.A., Auwerx, J., and Mangelsdorf, D.J. (2000). Molecular basis for feedback regulation of bile acid synthesis by nuclear receptors. Mol. Cell *6*, 507–515.

Marciano, D.P., Chang, M.R., Corzo, C.A., Goswami, D., Lam, V.Q., Pascal, B.D., and Griffin, P.R. (2014). The therapeutic potential of nuclear receptor modulators for treatment of metabolic disorders: PPARγ, RORs, and Rev-erbs. Cell Metab. *19*, 193–208.

Mataki, C., Magnier, B.C., Houten, S.M., Annicotte, J.S., Argmann, C., Thomas, C., Overmars, H., Kulik, W., Metzger, D., Auwerx, J., and Schoonjans, K. (2007). Compromised intestinal lipid absorption in mice with a liver-specific deficiency of liver receptor homolog 1. Mol. Cell. Biol. *27*, 8330–8339.

Meissner, M., Nijstad, N., Kuipers, F., and Tietge, U.J. (2010). Voluntary exercise increases cholesterol efflux but not macrophage reverse cholesterol transport in vivo in mice. Nutr. Metab. (Lond) *7*, 54.

Oosterveer, M.H., Mataki, C., Yamamoto, H., Harach, T., Moullan, N., van Dijk, T.H., Ayuso, E., Bosch, F., Postic, C., Groen, A.K., et al. (2012). LRH-1-dependent glucose sensing determines intermediary metabolism in liver. J. Clin. Invest. *122*, 2817–2826.

Out, C., Hageman, J., Bloks, V.W., Gerrits, H., Sollewijn Gelpke, M.D., Bos, T., Havinga, R., Smit, M.J., Kuipers, F., and Groen, A.K. (2011). Liver receptor homolog-1 is critical for adequate up-regulation of Cyp7a1 gene transcription and bile salt synthesis during bile salt sequestration. Hepatology *53*, 2075–2085.

Qin, J., Gao, D.M., Jiang, Q.F., Zhou, Q., Kong, Y.Y., Wang, Y., and Xie, Y.H. (2004). Prospero-related homeobox (Prox1) is a corepressor of human liver

receptor homolog-1 and suppresses the transcription of the cholesterol 7-alpha-hydroxylase gene. Mol. Endocrinol. *18*, 2424–2439.

Rosenson, R.S., Brewer, H.B., Jr., Davidson, W.S., Fayad, Z.A., Fuster, V., Goldstein, J., Hellerstein, M., Jiang, X.C., Phillips, M.C., Rader, D.J., et al. (2012). Cholesterol efflux and atheroprotection: advancing the concept of reverse cholesterol transport. Circulation *125*, 1905–1919.

Ryu, D., Seo, W.Y., Yoon, Y.S., Kim, Y.N., Kim, S.S., Kim, H.J., Park, T.S., Choi, C.S., and Koo, S.H. (2011). Endoplasmic reticulum stress promotes LIPIN2-dependent hepatic insulin resistance. Diabetes *60*, 1072–1081.

Schoonjans, K., Annicotte, J.S., Huby, T., Botrugno, O.A., Fayard, E., Ueda, Y., Chapman, J., and Auwerx, J. (2002). Liver receptor homolog 1 controls the expression of the scavenger receptor class B type I. EMBO Rep. *3*, 1181–1187.

Stein, S., Lohmann, C., Schäfer, N., Hofmann, J., Rohrer, L., Besler, C., Rothgiesser, K.M., Becher, B., Hottiger, M.O., Borén, J., et al. (2010). SIRT1 decreases Lox-1-mediated foam cell formation in atherogenesis. Eur. Heart J. *31*, 2301–2309.

Talamillo, A., Herboso, L., Pirone, L., Pérez, C., González, M., Sánchez, J., Mayor, U., Lopitz-Otsoa, F., Rodriguez, M.S., Sutherland, J.D., and Barrio, R. (2013). Scavenger receptors mediate the role of SUMO and Ftz-f1 in Drosophila steroidogenesis. PLoS Genet. *9*, e1003473.

Treuter, E., and Venteclef, N. (2011). Transcriptional control of metabolic and inflammatory pathways by nuclear receptor SUMOylation. Biochim. Biophys. Acta *1812*, 909–918.

Venteclef, N., Haroniti, A., Tousaint, J.J., Talianidis, I., and Delerive, P. (2008). Regulation of anti-atherogenic apolipoprotein M gene expression by the orphan nuclear receptor LRH-1. J. Biol. Chem. *283*, 3694–3701.

Venteclef, N., Jakobsson, T., Ehrlund, A., Damdimopoulos, A., Mikkonen, L., Ellis, E., Nilsson, L.M., Parini, P., Jänne, O.A., Gustafsson, J.A., et al. (2010). GPS2-dependent corepressor/SUMO pathways govern anti-inflammatory actions of LRH-1 and LXRbeta in the hepatic acute phase response. Genes Dev. *24*, 381–395.

Ward, J.D., Bojanala, N., Bernal, T., Ashrafi, K., Asahina, M., and Yamamoto, K.R. (2013). Sumoylated NHR-25/NR5A regulates cell fate during C. elegans vulval development. PLoS Genet. *9*, e1003992.

Weber, C., and Noels, H. (2011). Atherosclerosis: current pathogenesis and therapeutic options. Nat. Med. *17*, 1410–1422.

Yang, F.M., Pan, C.T., Tsai, H.M., Chiu, T.W., Wu, M.L., and Hu, M.C. (2009). Liver receptor homolog-1 localization in the nuclear body is regulated by sumoylation and cAMP signaling in rat granulosa cells. FEBS J. *276*, 425–436.